iScience

CellPress
OPEN ACCESS

Article

Potential of tellurite resistance in heterotrophic bacteria from mining environments

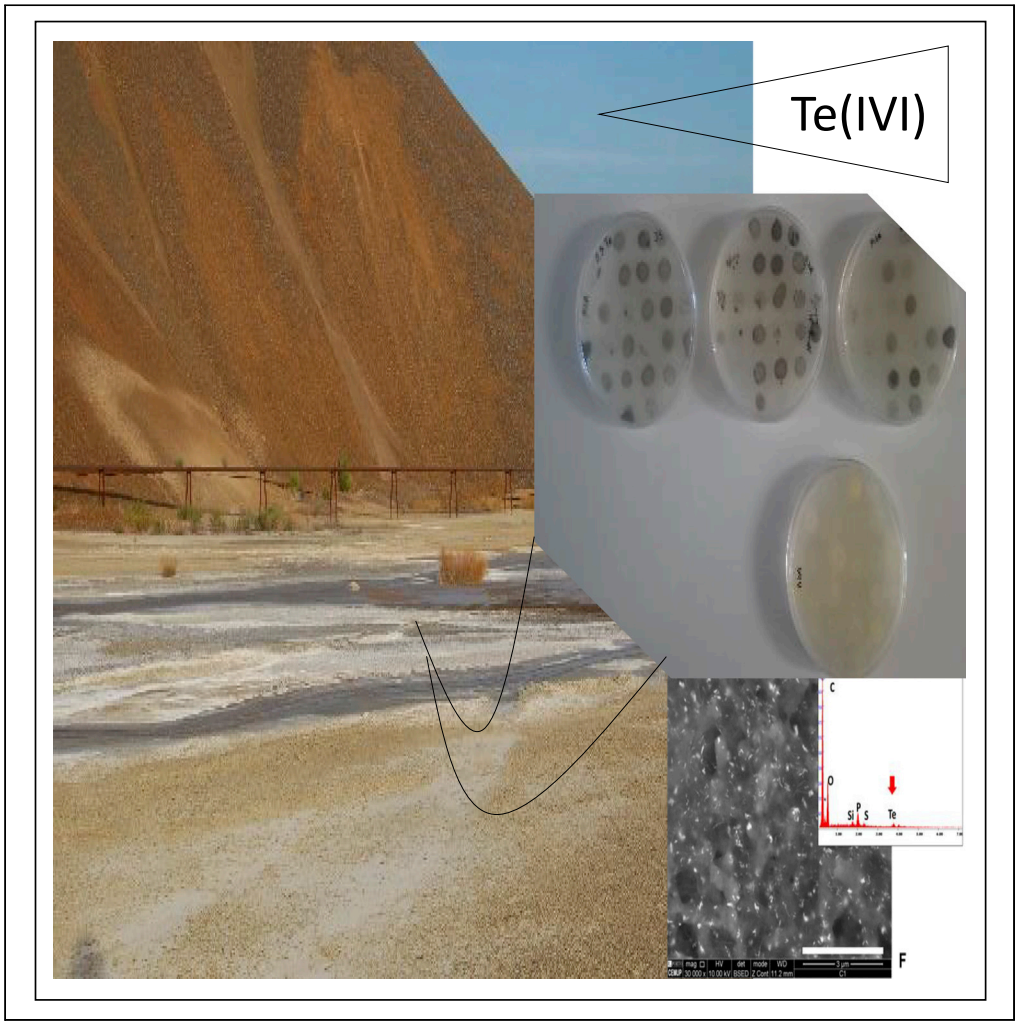

Pedro Farias,
Romeu Francisco,
Paula V. Morais

pvmorais@ci.uc.pt

Highlights

Sites with continuous high metal pressure as a source of Te-resistant bacteria diversity

Organism-specific Te (IV) reduction produces unique Te (0) insoluble structures

Unveiled Te resistance genetic determinants and arrangements in Bacillales

Farias et al., iScience 25, 104566
July 15, 2022
https://doi.org/10.1016/j.isci.2022.104566

iScience

CellPress
OPEN ACCESS

Article

Potential of tellurite resistance in heterotrophic bacteria from mining environments

Pedro Farias,[1] Romeu Francisco,[1] and Paula V. Morais[1,2,*]

SUMMARY

Untreated mining wastes and improper disposal of high-tech devices generate an environmental increase of bioavailable metalloids, exerting stress on autochthonous microbial populations. Tellurium is a metalloid, an element with raising economic importance; nevertheless, its interaction with living organisms is not yet fully understood. Here we characterized aerobic heterotrophic bacteria, isolated from high metal-content mining residues, able to resist/reduce tellurite into tellurium structures and to determine the presence of confirmed tellurite resistance genetic determinants in resistant strains. We identified over 50 tellurite-resistant strains, among 144 isolates, eight strains reduced tellurite to tellurium at different rates, with the concomitant production of tellurium deposits. Most tellurite resistance genes were found in strains from Bacillales, with the prevalence of genes of the *ter* operon. This work demonstrated that bacterial isolates, from environments with a persistent selective pressure, are potential candidates for uncovering strategies for tellurite resistance and/or production of valuable Te-containing materials.

INTRODUCTION

Tellurium, although rare in Earth's crust, is highly sought after in the field of nanotechnology (Mayers and Xia, 2002) owing to the combination of useful properties such as photoconductivity, nonlinear optical response, and relevant thermoelectric capacity. Te exists in nature mostly in five oxidation states, from those Te (IV) or Te (VI) is the most biologically relevant as both are soluble in water and therefore bioavailable. The latter anion is less soluble and less toxic than Te (IV) (Ollivier et al., 2011). Most studies have focused on the most soluble and toxic Te oxyanion, Te (IV), while the toxicity of the elemental form is yet to be determined. The increasing demand for Te will generate the production of components containing this metalloid, which, by reaching their end-of-life, will result in high-tech waste disposal. Improper disposal practices and waste management may create the conditions for Te leaching in the form of Te (IV) and Te (VI), which will seep into the surrounding environment, creating contaminated zones with niches subjected to high selective pressure (Kyle et al., 2011). The bactericidal activity of this metalloid was recognized before the use of antibiotics (Arenas et al., 2014), with a toxicity of the oxyanion tellurite occurring at concentrations as low as 8×10^{-6} M in *Escherichia coli* (Turner et al., 2012).

Biological tellurite resistance (Te^r) is not ubiquitous and occurs mainly by the reduction of the anionic form to a less toxic form. To this date, two reduction mechanisms have been described: the generation of the volatile di-methyl tellurite or the direct conversion to Te (0). The resistance to the reduction of Te (IV) to Te (0) can be mediated by several genetic mechanisms. Some are unspecific, such as nitrate-reductases (Sabaty et al., 2001) or other molybdopterin-containing enzymes (Theisen et al., 2013), and others are specific/semi-specific mechanisms.

To this date, although sometimes the mechanisms of resistance are not clear, a few genetic determinants have been linked to Te^r. An example of Te^r by methylation is the *tehAB* genetic system (Dyllick-Brenzinger et al., 2000), which confers moderate levels of resistance in *E. coli* K12, 1×10^3 M, this Te^r was also identified in *Haemophilus influenzae* (Taylor, 1999). In this system, the TehB protein has been identified as a methyltransferase. Te^r by reduction has been thoroughly explored in a *Rhodobacter* sp. strain possessing the *trgAB*/*cysK* determinants (Borghese et al., 2014, 2017). However, the genetic determinant conferring the highest Te^r is the *ter* operon. The *ter* operon was initially observed in plasmid pMER610 and R478 and contains seven genes (*terZABCDEF*). Within the core *ter* operon three main protein families are present, the

[1]University of Coimbra, Centre for Mechanical Engineering, Materials and Processes, Department of Life Sciences, 3000-456 Coimbra, Portugal

[2]Lead contact

*Correspondence: pvmorais@ci.uc.pt

https://doi.org/10.1016/j.isci.2022.104566

Table 1. Minimal Inhibitory Concentrations in solid and liquid R2A media, in the presence of Te (IV) of identified bacterial isolates from Panasqueira. Mathematical signals indicate growth compared to control situation: + - higher than control, ± - comparable to control and − - lesser than control

				Solid media				Liquid media		
					Te(IV) 10^{-3}mM				Te(IV) 10^{-3}mM	
				Control	0.5	1	3	Control	0.5	3
Pqanasqueira mine	Water	B2A1In2	*Rhodanobacter glycinis*	+	±	+	±	+	−	−
		B2A2W2	*Diaphorobacter polyhydroxybutyrativorans*	+	+	+	−	+	+	−
		B2A1Ga1	*Serratia glossinae*	+	+	+	±	+	−	−
	Basin 1 core sediments	B1S542 5W23	*Bacillus zhangzhouensis*	+	+	+	+	+	−	−
		B1S542 5W30	*Paenibacillus lupini*	+	+	+	−	+	−	−
		B1S542 10W27	*Bacillus aryabhattai*	+	+	+	−	+	−	−
		B1S542 5W4	*Bacillus toyonensis*	+	+	±	−	+	−	−
		B1S542 10W15	*Paenibacillus amylolyticus*	+	+	+	±	+	−	−
		B1S542 10W28	*Paenibacillus xylanexedens*	+	+	+	+	+	−	−
		B1S542 5W10	*Cellulomonas fimi*	+	+	+	+	+	−	−
		B1S422 2As4	*Cellulomonas cellasea*	+	±	±	±	+	+	−
		B1S542 10W16	*Bacillus simplex*	+	+	±	−	+	−	−
		B1S542 5W6	*Fictibacillus enclensis*	+	+	±	−	−	−	−
		B1S542 10W32	*Fontibacillus aquaticus*	+	+	±	−	−	−	−
		B1S522 10W5	*Paenibacillus xinjiangensis*	+	+	+	−	+	−	−
		B1S422 3W7	*Paenibacillus etheri*	+	±	±	−	+	−	−
		B1S542 5W33	*Paenibacillus sp.*	+	±	±	±	+	−	−
		B1S542 3W20	*Bacillus altitudinis*	+	+	+	−	+	−	−
		B1S532 10W7	*Paenibacillus sp.*	+	+	+	+	+	+	−
		B1S532 10W12	*Micrococcus aloeverae*	+	+	+	±	+	−	−
		B1S522 3W6	*Paenibacillus xinjiangensis*	+	+	+	−	+	−	−
		B1S422 3W5	*Paenibacillus etheri*	+	+	+	−	+	−	−
		B1S542 10W7	*Bacillus safensis*	+	+	+	+	+	+	+
		B1S542 3W19	*Bacillus altitudinis*	+	+	+	+	+	+	+
Panasqueira	Basin 2 core sediments	B2S342 2As5	*Bacillus altitudinis*	+	+	+	+	+	+	−
		B2S232 10W11	*Psychrobacillus psychrodurans*	+	±	±	−	+	−	−
		B2S342 10W7	*Tessaracoccus lapidicaptus*	+	±	±	−	+	−	−
		B2S322 2As8	*Flavihumibacter stibioxidans*	+	±	−	−	+	+	−
		B2S332 3W8	*Nocardioides pakistanensis*	+	±	±	±	+	−	−
		B2S322 2As7	*Cellulomonas cellasea*	+	−	±	±	−	−	−
		B2S232 10W1	*Bacillus simplex*	+	+	+	−	+	−	−
		B2S322 3W3	*Bacillus zhangzhouensis*	+	+	+	+	−	−	−
		B2S222 2As2	*Rhizobium selenitireducens*	+	±	±	±	+	−	−
		B2S322 5W2	*Cellulomonas cellasea*	+	±	±	±	+	+	−
		B2S322 3W14	*Cellulomonas cellasea*	+	±	±	±	+	−	−
		B2S222 5W24	*Bacillus zhangzhouensis*	+	+	+	+	+	+	−
		B2S232 10W3	*Actinotalea ferrariae*	+	+	+	+	+	−	−
		B2S322 10W11	*Cellulomonas cellasea*	+	±	±	±	+	−	−
		B2S222 10W19	*Mesorhizobium qingshengii*	+	+	+	+	+	−	−
		B2S222 2As20	*Cellulomonas cellasea*	+	±	±	±	+	−	−
		B2S222 5W10	*Cellulomonas marina*	+	±	±	−	+	+	−

(*Continued on next page*)

Table 1. *Continued*

		Solid media				Liquid media		
			Te(IV) 10^{-3}mM				Te(IV) 10^{-3}mM	
		Control	0.5	1	3	Control	0.5	3
B2S222 5W23	*Cellulomonas cellasea*	+	±	±	–	+	–	–
B2S322 2As13	*Cellulomonas cellasea*	+	±	±	±	+	–	–
B2S242 3W3	*Mesorhizobium qingshengii*	+	±	±	±	+	–	–
B2S232 Ga14	*Staphylococcus warneri*	+	±	+	–	+	–	–
B2S332 5W3	*Actinotalea ferrariae*	+	±	±	–	–	–	–
B2S222 2As1	*Cellulomonas cellasea*	+	+	+	±	+	+	–
B2S322 3W16	*Actinotalea ferrariae*	+	±	±	–	+	–	–

TerB, the TerC, and the TerD family. The three family proteins *terB*, *terC*, *terD*, and *terE* have been shown to be directly involved in Te^r (Turner et al., 1994). Several genetic arrangements of the *ter* operon have been identified among Actinobacteria, Firmicutes, and Gammaproteobacteria lineages (Anantharaman et al., 2014). In some of these genetic organizations, additional genes for Te^r are present, such as the genes encoding protein TelA and homologs (Franks et al., 2014). The only directly observable effect of Te^r determinants has been the extracellular deposition of Te-containing crystals in the vicinity of the outer membrane, with reduced intracellular Te bioaccumulation (Kormutakova et al., 2000). Early studies also link the *ter* operon to phage inhibition (Phi) and resistance to pore-forming colicins (PacB) in *E. coli*, (Taylor, 1999).

As verified for other metals, bioreduction leads to the formation of Te-containing intra-/extracellular nanostructures. Diversity of microorganisms has shown the capacity to form these nanostructures, such as *Enterobacter cloacae* (Contreras et al., 2018), *Ochrobactrum* sp. (Zonaro et al., 2017), *Shewanella* sp. (Vaigankar et al., 2018), and *Rhodobacter capsulatus* (Borghese et al., 2014, 2017). An increasing interest in understanding the formation of these structures is the result of the growing potential range of applications for bio-produced nanoparticles covering fields such as optical imaging (Plaza et al., 2016) or novel battery technology (Kim et al., 2015). Consequently, the isolation and characterization of organisms from a large number of different environments with potential for Te ions reduction gained importance, namely sea sediments (Csotonyi et al., 2006; Ollivier et al., 2008), fouled waters (Chien and Han, 2009), Antarctic samples (Arenas et al., 2014; Plaza et al., 2016), mine tailings (Maltman et al., 2015) among others. One environment of interest is mines and long-lasting mine tailings where the continuous selective pressure of multiple metals is present in the ecosystem. In our study, three mining sites were used to isolate microorganisms. Aljustrel is a site of a decommissioned old copper mine where sediments were collected from superficial tailings. These tailings were unaffected by human activity for many years but were subjected to environmental pressures. Panasqueira site is an active tungsten mine and the tailings where bacteria were isolated from are either old over 50 years, and still with high content of tungsten, or recent and with less concentration of target elements for mining. Sediments also vary in-depth and moisture content. Jales site is an exploratory test gallery in a region of gold deposits. Samples collected are superficial and mostly undisturbed by either human activity.

This study aims to reveal the diversity of Te^r responses of environmental strains, isolated from different mining sites, where the continuous presence of different mixtures of metals exerts selective pressure on the autochthonous microbial community. The Te (IV) reduction capacity of metabolically active isolates was determined by following Te (IV) depletion and by the visualization of the resulting Te insoluble particles. The presence of genetic determinants conferring resistance to Te (IV) was confirmed by targeted PCR.

RESULTS

Isolation, identification, and screening for tellurite-resistant bacteria

From the three sites sampled (Figure 1) a total of 144 different isolates were collected. From Panasqueira mine, 95 different isolates were recovered, 83 from cores of the tailings basins, 12 from the tailings surface waters. From the entire, identified, collection of Panasqueira microorganisms, 47 were resistant to 1×10^{-3} M Te (IV) and of these, 27 were resistant to the concentration of, at least, 3×10^{-3} M Te (IV) (Table 1). From

Table 2. Minimal Inhibitory Concentrations in solid and liquid R2A media, in the presence of Te (IV) of identified bacterial isolates from Aljustrel and Jales. Mathematical signals indicate growth compared to control situation: + - higher than control, ± - comparable to control and − - lesser than control

				Solid media				Liquid media		
					Te (IV) 10^{-3}M				Te (IV) 10^{-3}mM	
				Control	0.5	1	3	Control	0.5	3
Jalegallery	Sediments	Jales 26	*Sphingomonas alpina*	+	–	+	–	+	–	–
		Jales W30	*Mesorhizobium qingshengii*	+	±	±	–	–	–	–
		Jales As33	*Mycobacterium montmartrense*	+	+	±	–	+	–	–
		Jales As34	*Mycobacterium montmartrense*	+	+	+	±	+	–	–
		Jales 37	*Sphingomonas oligophenolica*	+	+	+	–	+	–	–
		Jales As35	*Mycobacterium montmartrense*	+	+	±	±	+	–	–
		Jales As7	*Paenibacillus borealis*	+	+	±	–	–	–	–
		Jales W48	*Mycobacterium gilvum*	+	+	±	±	+	–	–
		Jales 27	*Mesorhizobium qingshengii*	+	+	±	±	+	–	–
		Jales As8	*Sphingobium aromaticiconvertens*	+	±	±	±	+	–	–
		Jales As46	*Mesorhizobium qingshengii*	+	+	±	–	+	–	–
		Jales Te58	*Mesorhizobium qingshengii*	+	+	+	–	+	+	–
		Jales 44	*Okibacterium fritillariae*	+	±	±	±	+	–	–
		Jales Ga42	*Mycobacterium peregrinum*	+	+	+	–	+	–	–
		Jales As52	*Mesorhizobium qingshengii*	+	+	+	–	+	–	–
		Jales 40	*Mycobacterium sp.*	+	+	±	–	+	–	–
		Jales 51	*Hydrotalea flava*	+	±	±	–	+	–	–
		Jales 50	*Mesorhizobium qingshengii*	+	+	±	–	–	–	–
		Jales 21	*Mycobacterium fortuitum subsp. acetamidolyticum*	+	+	+	±	+	–	–
		Jales Ga6	*Curtobacterium flaccumfaciens*	+	±	–	±	+	+	–
		Jales Te55	*Mesorhizobium qingshengii*	+	+	±	±	+	+	+
		Jales 28	*Mesorhizobium qingshengii*	+	+	±	–	+	–	–
		Jales W3	*Bradyrhizobium cajani*	+	+	±	±	+	–	–
		Jales Te59	*Mesorhizobium qingshengii*	+	+	+	–	+	+	–
Aljustrel mine	Sediments	ALJ98a	*Bacillus mycoides*	+	+	+	+	+	+	+
		ALJ98b	*Paenibacillus tundrae*	+	+	+	+	+	+	+
		ALJ109b	*Paenibacillus sp.*	+	+	+	+	+	+	+

Jales samples, a total of 44 organisms were isolated in R2A agar and 24 were identified, from which 23 isolates were resistant to concentrations of 1 × 10^{-3} M Te (IV) and 9 to 3 × 10^{-3} M Te (IV). From Aljustrel the enrichment yielded five strains, of which three were able to grow in solid media spiked with concentrations of up to 5 × 10^{-3} M Te (IV) (Table 2).

Strains with MIC higher than 5 × 10^{-4} M Te (IV) were identified based on 16S rRNA gene sequence and phylogenetic relatedness with type strains from the NCBI database. The identification results grouped the strains into *Actinobacteria* (44.7%), *Firmicutes* (34.2%), and *Proteobacteria* (21.1%) phyla. The identified bacteria with MIC over 1 × 10^{-3} M Te (IV) were tested for increasing Te (IV) concentrations in liquid media. The most representative resistant organisms, with a MIC of 5 × 10^{-4} M Te (IV), belonged to the genera *Bacillus*, *Paenibacillus*, and *Cellulomonas* (Tables 1 and 2).

Growth kinetics in the presence of tellurite and reduction ability

The strains resistant to 5 × 10^{-4} M Te (IV) in liquid growth (Table 1) were selected for the evaluation of tellurite reduction. Twelve strains did not show an ability to remove Te (IV) from the media, as the same or

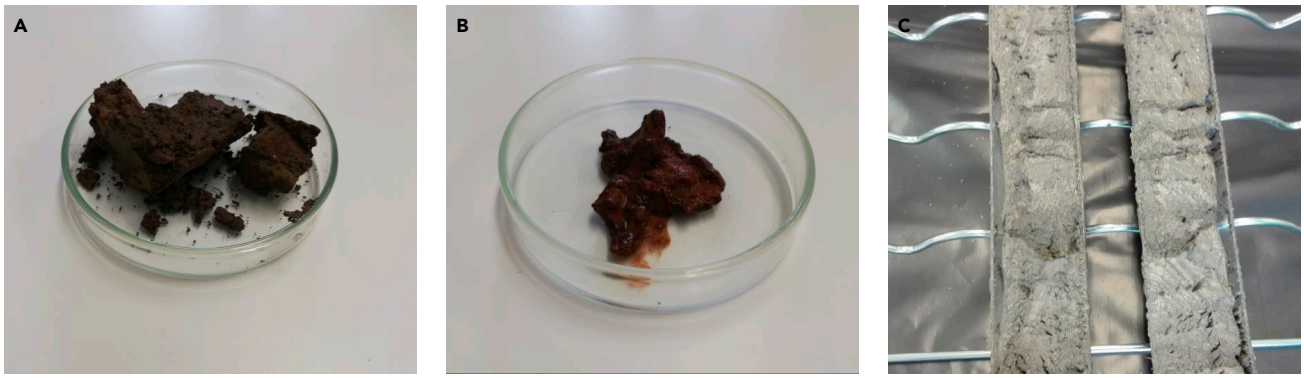

	Site Characteristics			Sediments Characteristics	
	Location	Activity state	Main product of mining activity	Moisture content	Dept
Aljustrel	37°52'07.3"N 8°09'24.7"W	Inactive	Copper	Slightly hydrated	2 to 4 m
Jales	40°07'32.71"N 7°42'51.18"W	Test gallery	Gold	Mixed (dry/wet	surface
Panasqueira	41°28'13.1"N 7°34'38.1"W	Active	Tungsten	Mostly hidrated /water samples	till 1 m

Figure 1. Mining isolation sources

Visual demonstration of biologically active sediments from (A) Aljustrel, (B) Jales, and (C) Panasqueira. Summarized the description of sampled mines and samples' general characteristics.

marginally different values of Te (IV), in solution, were detected throughout their growth. The eight remaining strains had their growth affected by Te (IV) (Figure 2). The specific growth rates of cells grown in 5 × 10^{-4} M Te (IV) were lower than the control culture, without Te (IV), for all eight strains (Figure 2). Strains *Paenibacillus pabuli* ALJ109b, *Bacillus mycoides* ALJ98a, *Paenibacillus taichungensis* ALJ98b and *Cellulomonas marina* strain B2S222 5W10 (5W10) maintained a growth rate similar to the control condition in concentrations up to 2.5 × 10^{-4} M Te (IV). *Bacillus safensis* strain B1S542 10W7 (10W7) increased its growth rate to 2.5 × 10^{-4} M of Te (IV), decreasing at the highest concentrations.

The strains that performed better at removing Te (IV) from liquid media were Panasqueira isolates *Bacillus altitudinis* strain B1S542 3W19 (3W19), *B. safensis* 10W7, and *C. marina* 5W10 (Figure 3) with Re values ranging from 6.03 to 4.39 $\Delta mg.DO^{-1}$ (Table 3). The isolates from Aljezur *B. mycoides* ALJ98a, *P. taichungensis* ALJ98b and *P. pabuli* ALJ109b showed moderate depletion efficiencies, with values ranging from 3.35 to 1.08 $\Delta mg.DO^{-1}$. Finally, the two Jales isolates *Mesorhizobium qingshengii* Jales Te59 and *Mesorhizobium qingshengii* Jales Te58 had the lowest depletion efficiencies, with reduction rates in the mid-hundreds of $\Delta\mu g.DO^{-1}$. The time required for each different strain to reach the late exponential phase was very distinct, ranging from 8 to 48 h. When considered, *B. altitudinis* 3W19 remained the highest performer with a reduction rate of 0.75 $\Delta mg.DO^{-1}.h^{-1}$, clearly higher than the second-best performer *B. safensis* 10W7, with a Rr of 0.23 $\Delta mg.DO^{-1}.h^{-1}$ (Table 3).

Tellurium aggregates production

Visual identification of Te-containing aggregates was performed by SEM with the identification of Te by coupled EDS for the six strains showing Re over 1 $mg.DO^{-1}$ and Rr over 0.05 $Re.h^{-1}$. These were prepared for SEM-EDS imaging as described in the methods section. Cell pellets of all strains revealed the presence of high-density deposits that by EDS were confirmed to have Te in varying abundances (Figure 3). *B. safensis* 10W7, *B. altitudinis* 3W19, and *C. marina* 5W10 formed shard or string-like Te-containing particles, white arrows in Figure 4, all other strains revealed Te-containing nanostructures with unclear geometries (Figure 4).

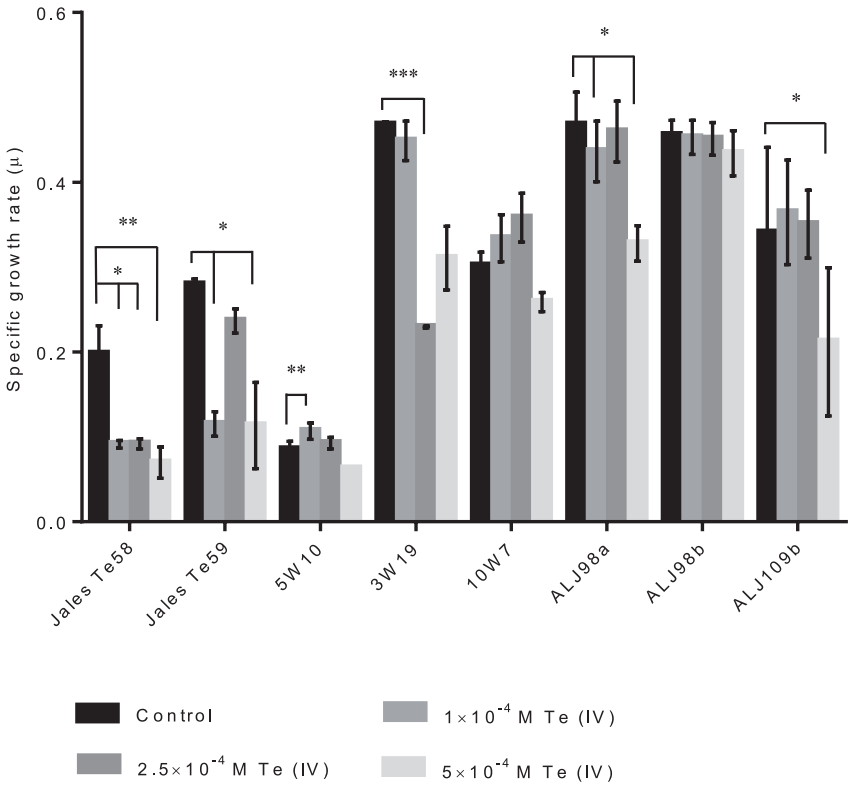

Figure 2. Growth in the presence of Te (IV)

Specific growth rates calculated for strains (left to right): *Mesorhizobium qingshengii* Te58, *Mesorhizobium qingshengii* Te59, *Cellulomonas marina* 5W10, *Bacillus altitudinis* 3W19, *Bacillus safensis* 10W7, *Bacillus mycoides* ALJ98a, *Paenibacillus tundrae* ALJ98b and *Paenibacillus pabuli* ALJ109b. Comparison of growth in selected concentration of Te (IV), Control (no Te (IV), 1×10^{-4} M Te (IV), 2.5×10^{-4} M Te (IV), and 5×10^{-4} M Te (IV) was conducted in triplicate, with standard deviations indicated in error bars. Statistical significance is represented by symbols *($p \leq 0.05$), **($p \leq 0.01$) and ***($p \leq 0.001$).

Screening for tellurite resistance genes

Resistance genes for Te (IV) were found in nine strains mostly belonging to the *Bacillus* genus. Gene *terZ* from the TerD family is the most ubiquitous in the strains tested being present in nine strains, *Bacillus altitudinis* 3W19, *Bacillus safensis* 10W7, *Paenibacillus pabuli* ALJ 109b, *Bacillus mycoides* ALJ 98a, *Mesorhizobium qingshengii* Jales Te55, *Cellulomonas marina* 5W10, *Flavihumibacter stibioxidans* B2S322 2As8 (2As8) and *Fictibacillus enclensis* B1S542 (5W6). Gene *telA* was present in four strains, *B. altitudinis* 3W19, *B. safensis* 10W7, *F. stibioxidans* 2As8, and *Bacillus zhangzhouensis* B2S222 5W24 (5W24). Both *terC* and *terD* were present in three strains each. Gene *terC* was found in *B. altitudinis* B1. S5. 4.2 3W19, *B. safensis* 10W7 and *B. zhangzhouensis* 5W24 and gene *terD* was found in *B. mycoides* ALJ 98a, *P. pabuli* ALJ 109b and *B. altitudinis* 3W19. Only one *terB* was found, in *B. altitudinis* 3W19. The strains with the highest number of resistance genes found were *B. altitudinis* 3W19 with *terD, terZ, terC,* and *telA*, followed by *B. safensis* B1. S5. 4.2 10W7 and *B. zhangzhouensis* 5W24 with *terZ, terC,* and *telA*. No positive amplicons were detected for genes *trgB* and *tehA* in mining isolates. All PCR products can be visualized in Figure S1.

Organization of the *ter* genetic determinants

Bacillus strains possessing more than one element of the *ter* gene cluster were considered for the determination of the arrangement of the constituting *ter* genes. From the eight combinations selected for *ter* genes arrangement only two produced amplicons. All amplicons produced were sequenced and an identification of the amplified region was presented for all the identifiable regions. The four strains tested had amplicons from *terZ* forward to *terC* reverse, contrarily only *B. subtilis* ALJ98a had an amplicon

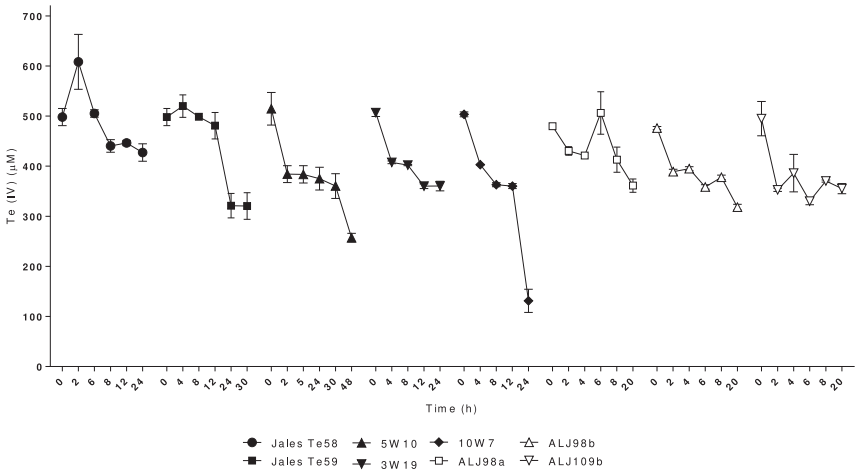

Figure 3. Tellurite depletion with environmental bacteria

Tellurite depletion from liquid media, over time, for strains able to grow in liquid media with 5×10^{-4} M Te (IV). Strains (left to right): Mesorhizobium qingshengii Te58, Mesorhizobium qingshengii Te59, Cellulomonas marina 5W10, *Bacillus altitudinis* 3W19, *Bacillus safensis* 10W7, *Bacillus mycoides* ALJ98a, *Paenibacillus tundrae* ALJ98b and *Paenibacillus pabuli* ALJ109b. Results are presented as the result of triplicates, with standard deviations indicated in error bars.

from *terC* forward to *telA* reverse (Figure 5). Fragment sizes from amplicon terZ-terC ranged from 1.4 kb to 2.9 kb, approximately, with amplicons in each strain varying in number and in size. In *B. mycoides* ALJ98a and *B. safensis* 10W7 only one amplicon resulted from the fragment *terZ-terC* PCR, of approximately 2.9 kb. PSI-Blast identified, in *B. safensis* 10W7, from 5′ to 3′, two TerD family protein/stress response protein (Id = 99.48%/Id = 99.49%) and one TerC family protein (Id = 98.98%). In *B. mycoides* ALJ98a, from 5′ to 3′, one TerD family protein (Id = 99.23%) and one TerC family protein (Id = 99%) (Figure 5 and Table 4). Both *B. altitudinis* 3W19 and *B. zhangzhouensis* 5W24 produced multiple fragments in terZ-terC PCR. Strain 3W19 produce a fragment of approximately 2.7 kb with, from 5′ to 3′, two TerD family protein (Id = 100%/Id = 99.23%) and one TerC family protein (Id = 99.45%). The smaller amplicon from strain 3W19 that was possible to sequence was 1.4 kb and was identified, from 5′ to 3′, one TerD family protein (Id = 100%) and one TerC (Id = 99.16%). Strain 5W24 produces a fragment of approximately 2.7 kb with, from 5′ to 3′, one VWA domain-containing protein (ID = 99.76%), one tellurium resistance protein TerD (Id = 100%), and one TerC/Alx family metal homeostasis membrane protein (Id = 100). The smaller amplicon from strain 5W24 that was possible to sequence was 2.1 kb and was identified, from 5′ to 3′, one tellurium resistance protein TerD (Id = 100%), one TerD family protein (Id = 99.35%), and one TerC/Alx family metal homeostasis membrane protein (Id = 100%) (Figure 5 and Table 4). The terC-telA amplicon obtained in strain ALJ98a was 2.9 kb in size and was identified, from 5′ to 3′, one TerC family protein (Id = 99.35%) and one toxic anion resistance protein (Id = 99.09) (Figure 5 and Table 4).

Table 3. Description of the reduction efficiency (Re) and reduction rate (Rr) for selected organism from three different mining sites

Organism	Origin	Re (Δmg/DO)	SD	Rr (mg/DO/h)	SD
Mesorhizobium qingshengii Jales Te58	Jales	0.88	0.31	0.04	0.013
Mesorhizobium qingshengii Jales Te59		0.52	0.04	0.02	0.001
Cellulomonas marina 5W10	Panasqueira	4.39	0.51	0.09	0.011
Bacillus altitudinis 3W19		6.03	0.12	0.75	0.005
Bacillus safensis 10W7		5.49	0.23	0.23	0.01
Bacillus mycoides ALJ98a	Aljezur	3.35	0.28	0.17	0.014
Paenibacillus tundrae ALJ98b		1.08	0.21	0.05	0.011
*Paenibacillus pabuli*ALJ109b		1.26	0.05	0.06	0.003

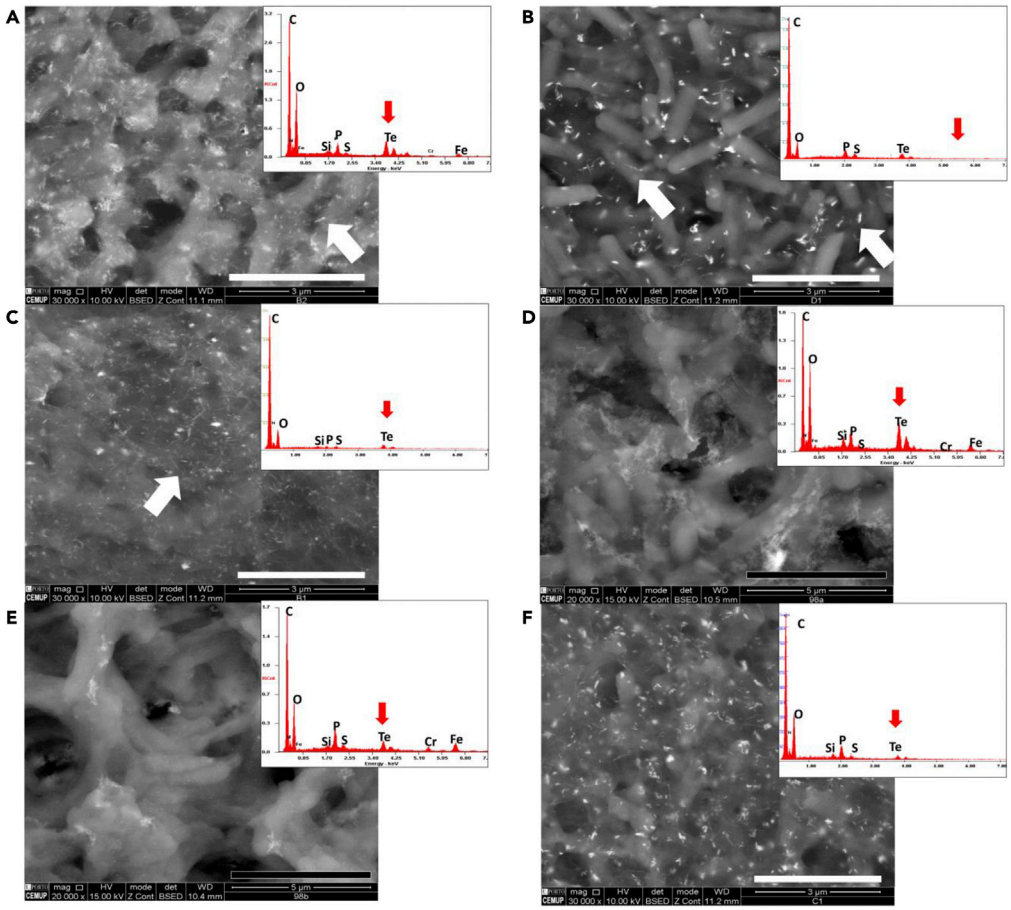

Figure 4. SEM micrographs of tellurite reducing cells fixated on stainless steel surfaces

(A) Cellulomonas marina 5W10, (B) *Bacillus altitudinis* 3W19, (C) *Bacillus safensis* 10W7, (D) *Bacillus mycoides* ALJ98a, (E) *Paenibacillus tundrae* ALJ98b,and (F) *Paenibacillus pabuli* ALJ109b. For images (D), (E) bar (black) = 5 μm; for images (A), (B), (C) and (F) bar (white) = 3 μm. High-density metal deposits are represented in white. EDS spectra are obtained from reads at randomly selected white segments and red arrows highlight Te detection in spectra. Inlets in SEM micrographs (white arrows) highlight organized features (described in the text).

DISCUSSION

The mining environments have characteristic elements that shape microbiome including pH, metal concentration/content, temperature, dissolved oxygen, and total organic carbon (Liu et al., 2014; Chung et al., 2019; Sibanda et al., 2019). The continuous exposure to a high concentration of different metals and low carbon selects for distinct microorganisms able to deal with such environments (Liu et al., 2019; Chung et al., 2019). All three sampled mining sites in this study had different features; in none of these Te was a target element for mining (Figure 1). As Te was not the metal extracted, discarded residues were expected to have relatively higher concentrations.

This work presents for the first time strains from the genera *Cellulomonas* and *Mesorhizobium*, as resistant to Te (IV). This opens a new possibility of study in Te^r mechanisms and genes. The overall diversity of Te (IV)-resistant bacteria was large with four different Phyla recovered from all three sampling sites (*Actinobacteria*, *Proteobacteria*, *Firmicutes*, and *Bacteroidetes*). The results indicate that, in these specific environments, *Mesorhizobium*, *Cellulomonas*, *Bacillus* and *Paenibacillus*, may be prevalent genera with high tolerance to the presence of Te (IV). In the Panasqueira site, the Te-resistant bacterial isolates recovered belong to some of the most abundant genera of the microbial community, as determined by metagenomic (Chung et al., 2019). As previously illustrated in an earlier microbial diversity study from this site *Bacillus* and *Cellulomonas* are two of the six genera composing the local core microbiome of the mine

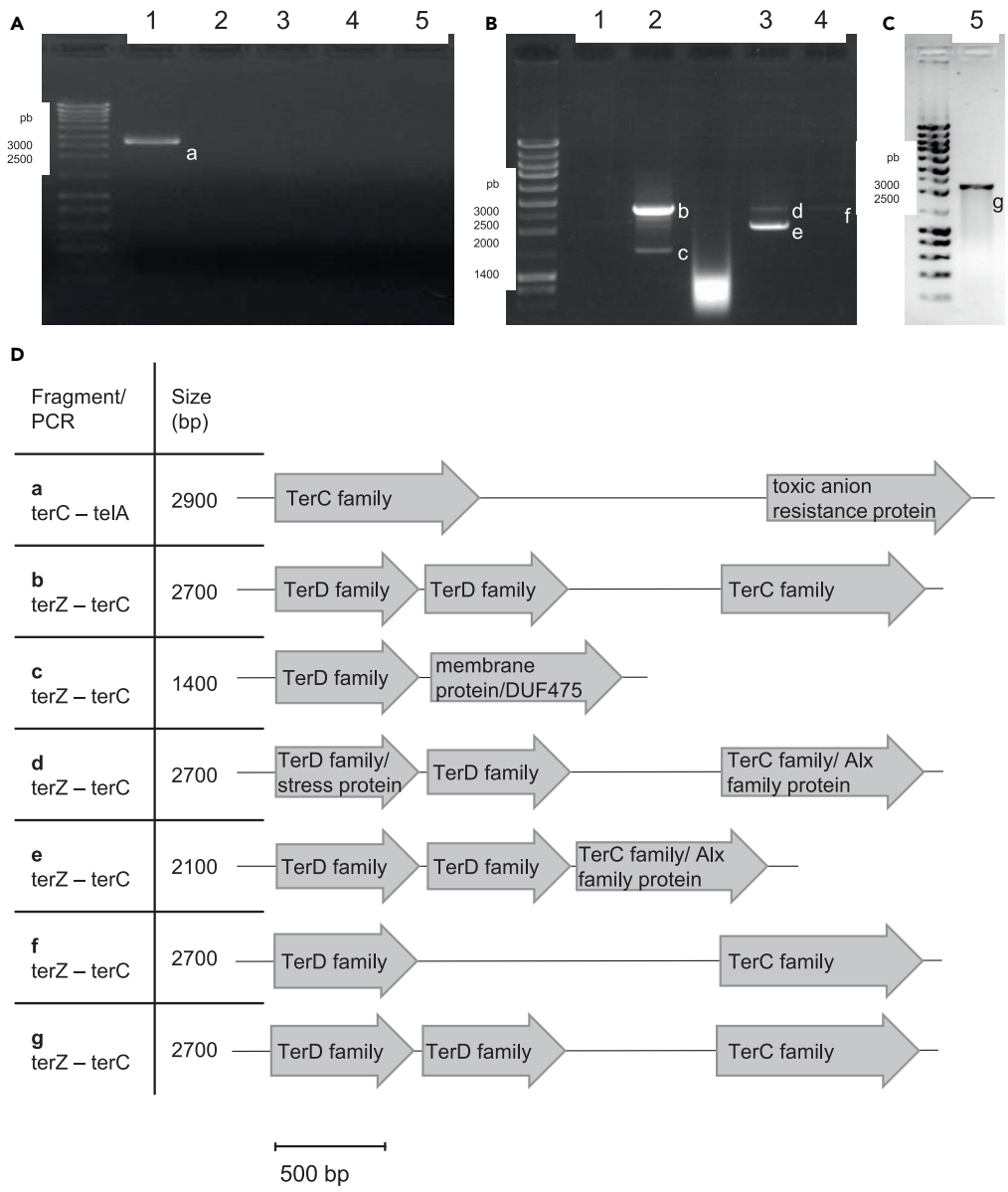

Figure 5. Genetic organization of *ter* gene clusters in *Bacillus* strains

PCR of multi-gene amplicons, identification of amplification products, and putative genetic arrangements.

(A) PCR of fragment *terC-telA*, 1. *Bacillus mycoides* ALJ98a, 2. *Bacillus zhangzhouensis* 5W24, 3. *Bacillus safensis* 10W7, 4. *Bacillus altitudinis* 3W19 and 5. Negative control.

(B and C) PCR of fragment *terZ-terC*: 1. Negative control, 2. *Bacillus altitudinis* 3W19, 3. *Bacillus zhangouensis* 5W24, 4. *Bacillus mycoides* ALJ98a and 5. *Bacillus safensis* 10W7.

(D) Diagram representation of genetic arrangement based on sequenced and identified amplicons **a** to **g**, with abbreviated identification. Size indication based on amplicon positioning on the gel.

tailings, with *Bacillus* representing the majority of the community of half the sampling sites (Chung et al., 2019). Most *Mesorhizobium* isolated, a common genus found in plant rhizobia, originated from samples of the Jales mining site. Unlike the Panasqueira mining site, the Jales gallery is not in operation since 1993 and was, therefore, not impacted by continuous human activity for several years, with the surrounding area being converted into agro/forestry areas. Considering the differences in samples' characteristics (Figure 1) and human activity on the isolation site it is expected to find variations in isolates recovered.

Table 4. Identification obtained by PSI-Blast of fragments indicated on Figure 5/bottom image, left to right

Amplicon	Blastx Identification	Assession number	Identity (%)
a	TerC family protein	WP_153252914.1	99.35
	toxic anion resistance protein	WP_098333049.1	99.09
b	TerD family protein	WP_007498343.1	100
	TerD family protein	WP_008342133.1	99.23
	TerC family protein	WP_007498342.1	99.45
c	TerD family protein	WP_039166394.1	100
	TerC family protein	WP_144556175.1	99.16
d	VWA domain-containing protein	WP_202671625.1	99.76
	Tellurium resistance protein TerD	WP_071681669.1	100
	TerC/Alx family metal homeostasis membrane protein	WP_024485071.1	100
e	Tellurium resistance protein TerD	WP_071681669.1	100
	TerD family protein	WP_141130909.1	99.35
	TerC/Alx family metal homeostasis membrane protein	WP_024485071.1	100
f	TerD family protein	WP_007498343.1	99.23
	TerC family protein	WP_144556175.1	99
g	Stress response protein SCP2	SDD49373.1	99.49
	TerD family protein	WP_025751616.1	99.48
	TerC family protein	WP_153252914.1	98.98

All identified fragments with coverage $E \leq 0.01$.

Tellurium ions resistance in *Bacillus* is usually related to their ability to reduce Te (IV), the oxyanion toxic form, to Te (0) (Franks et al., 2014). In *Paenibacillus*, although there are no publicly available reports concerning Te^r mechanisms, considering the phylogenetic proximity of the two taxa, likely resistant strains of *Paenibacillus* were also able to reduce Te (IV). Our previous study describes in detail the ability of *Paenibacillus pabuli* ALJ109b, from Aljustrel, to reduce Te (VI) using flagellin (Farias et al., 2021). Most of the recognized Te^r genetic determinants were not found in this strain, and those that were found did not display the usual organization of Te (IV) resistance gene clusters or operons.

The impact of Te (IV) on the growth of tested strains was mainly negative, decreasing growth with increasing Te (IV) concentrations, with few exceptions. Highest significant variations in the specific growth rate were mainly observed comparing the highest concentration of Te (IV), as expected. Low concentrations of Te (IV) significantly increased specific growth rates in *C. marina* 5W10 and this result is unexpected and not yet found in previous studies with other bacterial strains. Nevertheless, this variation was small in comparison to the other strains tested. The Te (IV) reduction capacity of metabolically active isolates was determined by following Te (IV) depletion and by the visualization of the resulting Te insoluble particles. In this work, bacterial strains demonstrated varied Te (IV) reducing performance, either calculating by cell mass or time, between strains. Isolates from Panasqueira mine *Bacillus altitudinis* 3W19, *Bacillus safensis* 10W7, and *Cellulomonas marina* 5W10 performed better than isolates from Aljustrel and Jales in reduction efficiency, mostly for the highest depletion values of Te (IV) in liquid media, no records were found in the literature of Te (IV) reduction by *Cellulomonas* strains. The reduction rate was also higher for strains *B. altitudinis* 3W19 and *B. safensis* 10W7 as well as for *Bacillus mycoides* ALJ98a, all these strains have high specific growth rates with small variation in growth, with 5×10^{-4} M Te (IV), compared to most other strains. Previous works demonstrated that *Bacillus* sp. strain STG-83 was able to reduce 50% of 1×10^{-3} M of Te (IV) in 104 h (Soudi et al., 2009), and a *Bacillus thermoamylovorans* strain SKC1 was able to completely reduce the 5×10^{-4} M of soluble Te (IV) in 10 days (Slobodkina et al., 2007). In this study, *Bacillus* strains are, from an application perspective, the best reducers, having highest Te (IV) depletion with less cell mass in shorter times. Despite the lack of comparative measurements in the literature, for the Te (IV)-Te(0) biologic conversion, the determination, in this study, of reduction efficiencies and reduction rates allows an efficient strategy to select strains able to manufacture Te structures. Absolute variations in Te (IV) depletion, seen in

Figure 3, points to *B. safensis* 10W7 as the best Te (IV) reducer by a two-fold difference compared to most strains tested. Moreover, the formation of Te precipitates was observed for selected strains. Most show a clear indication of the formation of Te (0) aggregates with different levels of structural organization. The formation of different structures of aggregates is indicative of different metabolic mechanisms involved in the formation of said structures, as is observed in previous works (Wang et al., 2018). The strain *B. altitudinis* 3W19 appears to produce two morphologically distinct Te-containing structures. The formation of string-like deposits of Te in the case of *B. safensis* 10W7 and *B. altitudinis* 3W19 is indicative of template base formation of nanoparticles on cell structures, i.e. the flagellum, like what is suggested for *P. pabuli* ALJ109b (Farias et al., 2021). Shard/rod-like structures, observed in *B. altitudinis* 3W19 and *C. marina* 5W10, were previously observed in *Pseudomonas putida* strain BS228 (Suzina et al., 1995), in *Pseudomonas pseudoalcaligenes* strain Te (Forootanfar et al., 2015) or in *Bacillus selenitireducens* and *Sulfurospirillum barnesii* (Baesman et al., 2007), indicating that these geometries are common in Te-containing nanostructures.

Most of the Te^r genes identified in the strains tested belonged to the TerD family, nine *terZ* and three *terD* according to our identification, despite PSI-Blast identification available only identified most genes as belonging to TerD family. Some genes from this family, *terD* paralogs, *terE,* and *terZ* are highly conserved among Firmicutes lineage (Anantharaman et al., 2014), hence the higher abundance in the strains tested, mostly from the *Bacillus* and *Paenibacillus* genus. The TerC family is also represented in the strains tested but the TerB family was not found. Considering that, in the strains tested, Te (IV) resistance involve the *ter* operon, this result is contrary to what is seen in the literature for several strains, namely *Escherichia coli* O 157:H17, where it was demonstrated that for Te^r, the genes *terB*, *terC*, *terD,* and *terE* were required (Taylor et al., 2002). This result is a variation on the known genetic organization of Te^r that may translate into a different resistance mechanism, albeit undefined as the *ter* Te^r mechanism is still unknown.

The study of the arrangement of genes from the *ter* operon in the strains possessing more than one gene revealed two possible organizations. *B. mycoides* ALJ98a indicated a structure similar to the *yceC* operon in *Bacillus subtilis* strain trpC2 attSPβ, with two *terD* family genes, a *terC* and a *telA*, only lacking the *yceG* upstream to *telA*. Contrarily, *B. altitudinis* 3W19, *B. safensis* 10W7, and *B. zahngouensis* 5W24 only share the initial structure with two/three *terD* family genes and a *terC*. Considering that *telA* was also present in these three strains, the genetic arrangement present seems more related to that of *Chitinophaga pinensis* DSM 2588 where the *terC-telA* region is interrupted by a biosynthetic module (Anantharaman et al., 2014). Only one amplicon of the gene *terB* was found, in *B. altitudinis* 3W19. TerB coding gene is more often found in *ter* arrangements that incorporate biosynthetic modules (Anantharaman et al., 2014). According to this author, the function attributed to TerB, is to link TerD and TerC either to the enzymes encoded by the biosynthetic module or to the diffusible product synthesized by them. The absence of *terB* in *B. safensis* 10W7 and *B. zhangzhouensis* 5W24 strains suggests an alternative *ter* system organization. In these strains un unidentified protein could be involved in TerD-TerC binding to biosynthetic module enzymes or its products, or the organisms does not require TerB owing to the absence of biosynthetic module.

In this work, we demonstrated that an organized cluster of *ter* determinants was present in strains with resistance to Te (IV) and demonstrated Te (IV) high reducing ability, except for the slow reducer *C. marina* 5W10. The relation between Te (IV) reduction and the existence of Te^r genetic determinants is visible in the *Bacillus* genera in mining isolates. The organization, as well as the components present in the *ter* gene cluster, is worthy of study to understand better why many variations of this gene cluster exist and how it affects Te^r.

Limitations of the study

This study uses exploratory PCR techniques to determine the presence of previously described Te (IV) resistance genes. Owing to a large number of bacterial strains and broad coverage of genera, families and orders the authors decided to use degenerate oligonucleotides that guaranteed amplification of desired genes from the maximum number of strains. This may have produced some false negatives for strains-containing genes with sequences not contemplated in the oligonucleotide design.

STAR★METHODS

Detailed methods are provided in the online version of this paper and include the following:

- KEY RESOURCE TABLE

SUPPLEMENTAL INFORMATION

Supplemental information can be found online at https://doi.org/10.1016/j.isci.2022.104566.

ACKNOWLEDGMENTS

This work was supported by the projects Biorecover under grant agreement nº 821096, funded by the European Union Horizon 2020, REVIVING – Revisiting mine tailings to innovate metals biorecovery – ERAMIN_2_67, MicroMiner - Microbiological technologies in the mining and recycling of high-tech critical metals – PTDC/CTA-AMB/31820/2017. This research is sponsored by FEDER funds through the program COMPETE and by national funds through FCT, under the project UID/EMS/00285/2020. Pedro Farias was supported by a grant from FCT (SFRH/BD/124091/2016). SEM-EDS analysis was performed at CEMUP, Porto, Portugal.

AUTHOR CONTRIBUTIONS

PF: Data curation, performed all benchwork, analyzed all data using bioinformatic and statistical analyses. Wrote the original draft. RF: Heading field sampling and processing of some analyses in the laboratory, assisting in strain isolations and growth and reduction assays. Reviewed the statistical analyses. Reviewed and edited article. PVM: Conceptualized whole experiment and secured funding. Supervised the laboratory, bioinformatics, and statistical analyses. Contribute to the original draft and revised article. All authors read and approved the article.

DECLARATION OF INTERESTS

The authors declare no competing interests.

Received: January 17, 2022
Revised: March 24, 2022
Accepted: June 6, 2022
Published: July 15, 2022

REFERENCES

Anantharaman, V., Iyer, L.M., and Aravind, L. (2014). Ter-dependent stress response systems: novel pathways related to metal sensing, production of a nucleoside-like metabolite, and DNA-processing. Molecular Biosystem *8*, 3142. https://doi.org/10.1039/c2mb25239b.

Arenas, F.A., Pugin, B., Henríquez, N.A., Arenas-Salinas, M.A., Díaz-Vásquez, W.A., Pozo, M.F., Muñoz, C.M., Chasteen, T.G., Pérez-Donoso, J.M., and Vásquez, C.C. (2014). Isolation, identification and characterization of highly tellurite- resistant, tellurite-reducing bacteria from Antarctica. Polar Science *8*, 40–52. https://doi.org/10.1016/j.polar.2014.01.001.

Baesman, S.M., Bullen, T.D., Dewald, J., Zhang, D., Curran, S., Islam, F.S., Beveridge, T.J., and Oremland, R.S. (2007). Formation of tellurium nanocrystals during anaerobic growth of bacteria that use Te oxyanions as respiratory electron acceptors. Appl. Environ. Microbiol. *73*, 2135–2143. https://doi.org/10.1128/AEM.02558-06.

Borghese, R., Baccolini, C., Francia, F., Sabatino, P., Turner, R.J., and Zannoni, D. (2014). Reduction of chalcogen oxyanions and generation of nanoprecipitates by the photosynthetic bacterium *Rhodobacter capsulatus*. J. Hazard Mater. *269*, 24–30. https://doi.org/10.1016/j.jhazmat.2013.12.028.

Borghese, R., Brucale, M., Fortunato, G., Lanzi, M., Mezzi, A., Valle, F., Cavallini, M., and Zannoni, D. (2017). Reprint of "Extracellular production of tellurium nanoparticles by the photosynthetic bacterium *Rhodobacter capsulatus*". J. Hazard Mater. *324*, 31–38. https://doi.org/10.1016/j.jhazmat.2016.11.002.

Chien, C.-C., and Han, C.-T. (2009). Tellurite resistance and reduction by a *Paenibacillus* sp. isolated from heavy metal-contaminated sediment. Environmental Toxicology Chemistry/SETAC *28*, 1627. https://doi.org/10.1897/08-521.1.

Chung, A.P., Coimbra, C., Farias, P., Francisco, R., Branco, R., Simão, F.V., Gomes, E., Pereira, A., Vila, M.C., Fiúza, A., et al. (2019). Tailings microbial community profile and prediction of its functionality in basins of tungsten mine. Sci. Rep. *9*, 19596. https://doi.org/10.1038/s41598-019-55706-6.

Contreras, F., Vargas, E., Jiménez, K., Muñoz-Villagrán, C., Figueroa, M., Vásquez, C., and Arenas, F. (2018). Reduction of gold (III) and tellurium (IV) by *Enterobacter cloacae* MF01 results in nanostructure formation both in aerobic and anaerobic conditions. Front. Microbiol. *9*, 3118. https://doi.org/10.3389/fmicb.2018.03118.

Csotonyi, J.T., Stackebrandt, E., and Yurkov, V. (2006). Anaerobic respiration on tellurate and other metalloids in bacteria from hydrothermal vent fields in the Eastern Pacific Ocean. Appl. Environ. Microbiol. *72*, 4950–4956. https://doi.org/10.1128/AEM.00223-06.

Dyllick-Brenzinger, M., Liu, M., Winstone, T.L., Taylor, D.E., and Turner, R.J. (2000). The role of cysteine residues in tellurite resistance mediated by the TehAB determinant. Biochem. Biophys. Res. Commun. *277*, 394–400. https://doi.org/10.1006/bbrc.2000.3686.

Farias, P., Francisco, R., Maccario, L., Herschend, J., Piedade, A.P., Sørensen, S., and Morais, P.V. (2021). Impact of tellurite on the metabolism of *Paenibacillus pabuli* AL109b with flagellin production explaining high reduction capacity. Front. Microbiol. *12*, 718963. https://doi.org/10.3389/fmicb.2021.718963.

Forootanfar, H., Amirpour-Rostami, S., Jafari, M., Forootanfar, A., Yousefizadeh, Z., and Shakibaie, M. (2015). Microbial-assisted synthesis and evaluation the cytotoxic effect of tellurium nanorods. Mater. Sci. Eng. C *49*, 183–189. https://doi.org/10.1016/j.msec.2014.12.078.

Franks, S.E., Ebrahimi, C., Hollands, A., Okumura, C.Y., Aroian, R.V., Nizet, V., and McGillivray, S.M. (2014). Novel role for the *yceGH* tellurite resistance genes in the pathogenesis of Bacillus anthracis. Infect. Immun. *82*, 1132–1140. https://doi.org/10.1128/IAI.01614-13.

Kanz, C., Aldebert, P., Althorpe, N., Baker, W., Baldwin, A., Bates, K., Browne, P., van den Broek, A., Castro, M., Cochrane, G., and Duggan, K. (2005). The EMBL nucleotide sequence database. Nucleic Acids Res. *33*, D29–D33. (Database issue). https://doi.org/10.1093/nar/gki098.

Kim, M.G., Kim, D.H., Kim, T., Park, S., Kwon, G., Kim, M.S., Shin, T.J., Ahn, H., and Hur, H.G. (2015). Unusual Li-ion storage through anionic redox processes of bacteria-driven tellurium nanorods. J. Mater. Chem. *3*, 16978–16987. https://doi.org/10.1039/C5TA04038H.

Kormutakova, R., Klucar, L., and Turna, J. (2000). DNA sequence analysis of the tellurite-resistance determinant from clinical strain of *Escherichia coli* and identification of essential genes. Biometals *13*, 135–139. https://doi.org/10.1023/A:1009272122989.

Kyle, J.H., Breuer, P., Bunney, K., Pleysier, R., and May, P. (2011). Review of trace toxic elements (Pb, Cd, Hg, As, Sb, Bi, Se, Te) and their deportment in gold processing. Part 1: mineralogy, aqueous chemistry and toxicity. Hydrometallurgy *107*, 91–100. https://doi.org/10.1016/j.hydromet.2011.01.010.

Liu, B., Su, G., Yang, Y., Yao, Y., Huang, Y., Hu, L., Zhong, H., and He, Z. (2019). Vertical distribution of microbial communities in chromium-contaminated soil and isolation of Cr(**VI**)-Reducing strains. Ecotoxicol. Environ. Saf. *180*, 242–251. https://doi.org/10.1016/j.ecoenv.2019.05.023.

Liu, J., Hua, Z.S., Chen, L.X., Kuang, J.L., Li, S.J., Shu, W.S., and Huang, L.N. (2014). Correlating microbial diversity patterns with geochemistry in an extreme and heterogeneous environment of mine tailings. Appl. Environ. Microbiol. *80*, 3677–3686. https://doi.org/10.1128/AEM.00294-14.

Maltman, C., Piercey-Normore, M.D., and Yurkov, V. (2015). Tellurite-tellurate-and selenite-based anaerobic respiration by strain CM-3 isolated from gold mine tailings. Extremophiles *19*, 1013–1019. https://doi.org/10.1007/s00792-015-0776-8.

Mayers, B., and Xia, Y. (2002). Formation of tellurium nanotubes through concentration depletion at the surfaces of seeds. Adv. Mater. *14*, 279–282. https://doi.org/10.1002/1521-4095(20020219)14:4<279::AID-ADMA279>3.0.CO;2.

Nielsen, P., Fritze, D., and Priest, F.G. (1995). Phenetic diversity of alkaliphilic *Bacillus* strains: proposal for nine new species. Microbiology *141*, 1745–1761. https://doi.org/10.1099/13500872-141-7-1745.

Ollivier, P.R.L., Bahrou, A.S., Marcus, S., Cox, T., Church, T.M., and Hanson, T.E. (2008). Volatilization and precipitation of tellurium by aerobic, tellurite-resistant marine microbes. Appl. Environ. Microbiol. *74*, 7163–7173. https://doi.org/10.1128/AEM.00733-08.

Ollivier, P.R.L., Bahrou, A.S., Church, T.M., and Hanson, T.E. (2011). Aeration controls the reduction and methylation of tellurium by the aerobic, tellurite-resistant marine yeast *Rhodotorula mucilaginosa*. Appl. Environ. Microbiol. *77*, 4610–4617. https://doi.org/10.1128/AEM.00351-11.

Plaza, D.O., Gallardo, C., Straub, Y.D., Bravo, D., and Pérez-Donoso, J.M. (2016). Biological synthesis of fluorescent nanoparticles by cadmium and tellurite resistant Antarctic bacteria: exploring novel natural nanofactories', *Microbial Cell Factories*. BioMed Central *15*, 76. https://doi.org/10.1186/s12934-016-0477-8.

Rainey, F.A., Ward-Rainey, N., Kroppenstedt, R.M., and Stackebrandt, E. (1996). The genus *Nocardiopsis* represents a phylogenetically coherent taxon and a distinct actinomycete lineage: proposal of *Nocardiopsaceae* fam. nov. Int. J. Syst. Bacteriol. *46*, 1088–1092.

Rutherford, K., Parkhill, J., Crook, J., Horsnell, T., Rice, P., Rajandream, M.A., and Barrell, B. (2000). Artemis: sequence visualization and annotation. Bioinformatics *16*, 944–945. http://www.ncbi.nlm.nih.gov/pubmed/11120685.

Sabaty, M., Avazeri, C., Pignol, D., and Vermeglio, A. (2001). Characterization of the reduction of selenate and tellurite by nitrate reductases. Appl. Environ. Microbiol. *67*, 5122–5126. https://doi.org/10.1128/AEM.67.11.5122-5126.2001.

Sibanda, T., Selvarajan, R., Msagati, T., Venkatachalam, S., and Meddows-Taylor, S. (2019). Defunct gold mine tailings are natural reservoir for unique bacterial communities revealed by high-throughput sequencing analysis. Sci. Total Environ. *650*, 2199–2209. https://doi.org/10.1016/j.scitotenv.2018.09.380.

Slobodkina, G.B., Bonch-Osmolovskaya, E.A., and Slobodkin, A.I. (2007). Reduction of chromate, selenite, tellurite, and iron (III) by the moderately thermophilic bacterium *Bacillus thermoamylovorans* SKC1. Microbiology *76*, 530–534. https://doi.org/10.1134/S0026261707050037.

Soudi, M.R., Ghazvini, P.T.M., Khajeh, K., and Gharavi, S. (2009). Bioprocessing of seleno-oxyanions and tellurite in a novel *Bacillus* sp. strain STG-83: a solution to removal of toxic oxyanions in presence of nitrate. J. Hazard Mater. *165*, 71–77. https://doi.org/10.1016/j.jhazmat.2008.09.065.

Suzina, N.E., Duda, V.I., Anisimova, L.A., Dmitriev, V.V., and Boronin, A.M. (1995). Cytological aspects of resistance to potassium tellurite conferred on *Pseudomonas* cells by plasmids. Arch. Microbiol. *163*, 282–285. https://doi.org/10.1007/BF00393381.

Taylor, D.E. (1999). Bacterial tellurite resistance. Trends Microbiol. *7*, 111–115. https://doi.org/10.1016/S0966-842X(99)01454-7.

Taylor, D.E., Rooker, M., Keelan, M., Ng, L.K., Martin, I., Perna, N.T., Burland, N.T.V., and Blattner, F.R. (2002). Genomic variability of O islands encoding tellurite resistance in enterohemorrhagic *Escherichia coli* O157:H7 Isolates. J. Bacteriol. *184*, 4690–4698. https://doi.org/10.1128/JB.184.17.4690-4698.2002.

Theisen, J., Zylstra, G.J., and Yee, N. (2013). Genetic evidence for a molybdopterin-containing tellurate reductase. Appl. Environ. Microbiol. *79*, 3171–3175. https://doi.org/10.1128/AEM.03996-12.

Turner, R.J., Borghese, R., and Zannoni, D. (2012). Microbial processing of tellurium as a tool in biotechnology. Biotechnology Advances *30*, 954–963. https://doi.org/10.1016/j.biotechadv.2011.08.018.

Turner, R.J., Weiner, J.H., and Taylor, D.E. (1992). Use of diethyldithiocarbamate for quantitative determination of tellurite uptake by bacteria. Anal. Biochem. *204*, 292–295. http://www.ncbi.nlm.nih.gov/pubmed/1332532.

Turner, R.J., Weiner, J.H., and Taylor, D.E. (1994). In vivo complementation and site-specific mutagenesis of the tellurite resistance determinant *kilAtelAB* from IncPα plasmid RK2Te(r). Microbiology *140*, 1319–1326. https://doi.org/10.1099/00221287-140-6-1319.

Vaigankar, D.C., Vaigankar, D.C., Dubey, S.K., Mujawar, S.Y., D'Costa, A., and Shyama, S.K. (2018). Tellurite biotransformation and detoxification by *Shewanella baltica* with simultaneous synthesis of tellurium nanorods exhibiting photo-catalytic and anti-biofilm activity. Ecotoxicol. Environ. Saf. *165*, 516–526. https://doi.org/10.1016/j.ecoenv.2018.08.111.

Wang, Z., Bu, Y., Zhao, Y., Zhang, Z., Liu, L., and Zhou, H. (2018). Morphology-tunable tellurium nanomaterials produced by the tellurite-reducing bacterium *Lysinibacillus* sp. ZYM-1. Environ. Sci. Pollut. Control Ser. *25*, 20756–20768. https://doi.org/10.1007/s11356-018-2257-y.

Yoon, S.-H., Ha, S.M., Kwon, S., Lim, J., Kim, Y., Seo, H., and Chun, J. (2017). Introducing EzBioCloud: a taxonomically united database of 16S rRNA gene sequences and whole-genome assemblies. Int. J. Syst. Evol. Microbiol. *67*, 1613–1617. https://doi.org/10.1099/ijsem.0.001755.

Zonaro, E., Piacenza, E., Presentato, A., Monti, F., Dell'Anna, R., Lampis, S., and Vallini, G. (2017). *Ochrobactrum* sp . MPV1 from a dump of roasted pyrites can be exploited as bacterial catalyst for the biogenesis of selenium and tellurium nanoparticles. Microbial Cell Factories. BioMed Central *16*, 215. https://doi.org/10.1186/s12934-017-0826-2.

STAR★METHODS

KEY RESOURCE TABLE

REAGENT or RESOURCE	SOURCE	IDENTIFIER
Bacterial strains		
Bacillus safensis strain B1S542 10W7	This study	UCCCB 133
Bacilus mycoides strain ALJ98a	This study	UCCCB 134
Mesorhizobium qingshengii strain Jales Te58	This study	UCCCB 135
Mesorhizobium qingshengii strain Jales Te59	This study	UCCCB 136
Bacillus zhangouensis strain B2S222 5W24	This study	UCCCB 137
Paenibacillus tundrae strain ALJ98b	This study	UCCCB 138
Bacillus altitudinis strain B1S542 3W19	This study	UCCCB 87
Cellulomonas marina strain B2S222 5W10	This study	UCCCB 86
Paenibacillus pabuli strain ALJ109b	Farias et al.2021	UCCCB 89
Chemicals, peptides, and recombinant proteins		
Reasoners 2A agar (R2A)	VWR	84671.0500
Luria Bertani (LB)	NZYTech	MB14501
Sodium tellurite	Sigma	400688-10G
Diethyl-di-thiocarbamate	Sigma	228680-5G
Critical commercial assays		
Gel purification kit	EZNA, VWR	D2500-02
Oligonucleotides		
Primers for "Screening for tellurite resistance genes" See Supplementary Material S1 Primers for "Organization of the ter genetic determinants" See Supplementary Material S1	This paper	N/A
Deposited data		
16S rRNA sequencing data from all samples	This study; Genbank	accession numbers from OK644207 to OK644280
ter determinants sequencing data	This study; Genbank	accession numbers from OL344531-OL344548
Software and algorithms		
MegaX	MEGA software	https://www.megasoftware.net/
EzBioCloud 16S rRNA gene sequence database v. PKSSU4.0	ChunLab; Kim et al., 2015; Yoon et al. (2017)	https://help.ezbiocloud.net/mtp-pipeline/; https://doi.org/10.1099/ijs.0.038075-0 https://doi.org/10.1099/ijsem.0.001755
IDFix	SAMx	http://www.samx.com/microanalysis/products/idfix_us.html
Prism	GraphPad software	https://www.graphpad.com/scientific-software/prism/
Other		
Infinite® 200 PRO Fluorimeter	Tecan Instruments	https://lifesciences.tecan.com/plate_readers/infinite_200_pro
FEI Quanta 400FEG	ThermoFisher Scientific	N/A
INCA Energy 350	Oxford Instruments	N/A

RESOURCE AVAILABILITY

Lead contact

Further information and requests for resources and reagents should be directed to and will be fulfilled by the lead contact, Paula V Morais (pvmorais@ci.uc.pt).

Materials availability

Strains of interest, used in this study, were deposited in the UCCCB culture collection under the identifiers: *Cellulomonas marina* B2S222 5W10 (UCCCB 86), *Bacillus altitudinis* B1S542 3W19 (UCCCB 87), *Paenibacillus pabuli* ALJ109b (UCCCB 89), *Bacillus safensis* B1S542 10W7 (UCCCB 133), *Bacilus mycoides* ALJ98a (UCCCB 134), *Mesorhizobium qingshengii* Jales Te58 (UCCCB 135), *Mesorhizobium qingshengii* Jales Te59 (UCCCB 136), *Bacillus zhangouensis* B2S222 5W24 (UCCCB 137) and *Paenibacillus tundrae* ALJ98b (UCCCB 138).

Data and code availability

All data supporting findings of this study are provided within the manuscript and its supplemental information section. Whole 16S rRNA sequencing data of strains has been deposited on the Genbank repository, under accession numbers from OK644207 to OK644280. Partial and whole sequencing data of *ter* determinants has been deposited on the Genbank repository, under accession numbers from OL344531-OL344548.

EXPERIMENTAL MODEL AND SUBJECT DETAILS

Sample collection

Sediment samples were collected from two mining sites the Aljustrel copper mine (37°52′07.3″N 8°09′24.7″W), in southern Portugal, and the Panasqueira tungsten mine (40°07′32.71″N, 7°42′51.18″W), in central Portugal. Additionally, a test gallery for gold mining, in Jales north Portugal (41°28′13.1″N 7°34′38.1″W). All sites have unique characteristics (see Figure 1 for sample/site description). Aljustrel samples were recovered by digging 1 m deep, into the discarded material of the sedimentary basin. Samples from Panasqueira were collected at 2 and 4 m from boreholes, using a dynamic geotool probe and a 50 mm poly-vinyl carbonate sampler with a diameter of 50 mm. Between each core sampling (B2S2, B2S3, B1S4 and B1S5) the sampler was decontaminated using 70% ethanol. Jales disturbed samples were collected from the walls of the gallery. All samples were collected and transported in sterile containers. Sediment samples were broken apart, homogenized and partitioned for further studies.

METHOD DETAILS

Bacterial strains isolation and growth

The bacterial isolation protocol targeted aerobic heterotrophic bacterial strains from sediments from all isolation sites. Aliquots from sediment samples, Panasqueira and Jales mining sites, were collected and serial dilutions were prepared, with saline solution (NaCl 0.85%) for inoculation of Reasoner 2A (R2A) agar (NZYTech, Portugal). Plates were incubated at 25°C for up to one month. Pure isolates were obtained from repeated streaking of a selection of colonies with different morphology and preserved at −80°C in growth media containing 15% glycerol.

Sediment samples from Aljustrel mining site were suspended in 50% diluted Luria Bertani (LB) medium (Sigma). The samples were incubated at 25°C for 7 days in an orbital shaker. Timely increments of sodium tellurite (Sigma) were added to the cultures, increasing from 5×10^{-4} M, 1×10^{-3} M, 3×10^{-3} M, 5×10^{-3} M up to 1×10^{-2} M. Prior to each Te (IV) enrichment, an aliquot of the suspension was plated in 50% diluted LB agar for selection of isolates, as described above.

DNA extraction, 16S rRNA gene amplification and identification

DNA from each isolate was obtained using the standard freeze-thaw method (Nielsen et al., 1995). Amplification of the nearly full-length 16S rRNA gene sequence was performed by PCR with universal primers (Rainey et al., 1996), (see Supplementary Table S1 for PCR conditions). The resulting amplicons, sequenced by Sanger method (Stabvida) were matched with the existing sequences using a nBlast search against the reference type strain database on the EzTaxon portal (Rutherford et al., 2000; Kanz et al., 2005).

Isolates metal resistance determination and growth

Metal resistance of the isolates was determined by minimal inhibitory concentration (MIC). Strains were grown in R2A agar (Jales and Panasqueira isolates) and LB agar (Aljustrel isolates), with increasing concentrations of Te (IV), 5×10^{-4} M, 1×10^{-3} M and 3×10^{-3} M. All bacterial growth was performed with incubation at 25°C for 24 to 48 h.

For the determination of specific growth rates, each isolate was grown in increasing concentrations of Te (IV), 1×10^{-4} M, 2.5×10^{-4} M and 5×10^{-4} M in LB and R2A broth, while comparing against growth in the absence of Te (IV). Growth kinetics were determined by evaluation of optical density (OD) variation (Abs 600 nm) of bacterial strains grown at 25°C, 100 rpm. Specific growth rates were determined for each strain at each concentration considering all values obtained at timepoints between early exponential and late exponential/early stationary phases (growth curves not shown).

Tellurite bio-reduction from liquid media

Tellurite reduction was evaluated in R2A for Jales and Panasqueira isolates and in LB for Aljustrel isolates, at the concentrations of 1×10^{-4} M, 2.5×10^{-4} M, 5×10^{-4} M. Aliquots for Te (IV) reduction testing were recovered at four points, as lag/early exponential, mid-exponential, late exponential and late stationary growth phase. After growth, cells were centrifuged for 20 min at 4000 g, the pellets were preserved for further tests and the supernatant was stored for evaluation of Te (IV) reduction. Quantitative depletion of Te (IV) was evaluated using a chromophore Diethyl-di-thiocarbamate (DDTC) method adapted from Turner and colleagues (Turner et al., 1992). The reagent mixture was prepared with 1 mM DDTC, Tris-HCl pH7 buffer and each sample was incubated for no more than 15 min prior to absorbance reading at 340 nm in an Infinite® 200 PRO fluorimeter. Quantitative data was obtained from a minimum of three experimental replicates.

The efficiency of Te (IV) depletion, Reduction efficiency (Re), was determined as the ratio of the absolute variation of Te (IV) in grams, from time 0 (T0) to late exponential growth (Tf), per growth, expressed as a variation on optical density, Tf – T0. Reduction rate (Rr) was determined as reason of the Re per time at Tf, as demonstrated in the equation.

$$Re = \frac{|\Delta Te|}{\Delta DO(Tf - T0)} \quad Rr = Re/t(Tf)$$

Tellurium aggregates production

Demonstration of Te precipitation was performed by scanning electron microscopy with coupled energy-dispersive X-ray spectroscopy (SEM-EDS) on samples of cells recovered from a late exponential phase in the presence of 5×10^{-4} M of Te (IV). Cell pellets from cultures were collected by centrifugation at 4000 *g*, washed twice in cold saline phosphate buffer (PBS), and resuspended in 0.1 mL of the same buffer. Droplets of cell concentrate ≈30 μL were dried in a 5 × 5 mm stainless steel plate, at room temperature, followed by two-step fixation with 2.5% glutaraldehyde followed by desiccation with increasing ethanol concentration, 70/80/90/95%. SEM micrographs were obtained on a FEI Quanta 400FEG ESEM and EDS analysis was accomplished using an Oxford INCA Energy 350 equipped with the SAMX IDIFIX software, with an accelerating voltage of 15 kV and a beam current of 20 nÅ.

Screening for tellurite resistance genes

DNA from each isolate was obtained as described in section "DNA extraction, 16S rRNA gene amplification and identification". Targeted genes for screening were selected based on proven demonstration of conferring Te (IV) resistance (BacMet used for reference) with preference given to genes conferring resistance with absolute or narrow specificity to Te ions. Oligonucleotide design was conducted considering, at least, inter-genus genetic homology, between selected strains to reduce degeneracy (see Supplementary Table S1 for oligonucleotide details and PCR conditions). Amplification of *terB* gene using primers dterB_F and dterB_R with annealing 45 s, 55°C; elongation 30 s, 72°C; *terD* gene using primers terD_F and terD_R with annealing 45 s, 50°C; elongation 1 min, 72°C; *terZ* gene using primers yceD_F and yceD_R with annealing 1 min, 58°C; elongation 1 min, 72°C; *terC* gene using primers yceF_F and yceF_R with annealing 1 min, 54°C; elongation 1 min, 72°C and *telA/yceH* gene using primers yceH_F and yceH_R with annealing 1 min, 57°C; elongation 1 min, 72°C and *tehA* gene using primers tehA_F and tehA_R with annealing 1 min, 50°C; elongation 1 min, 72°C. PCR amplicons were observed on a 1% agarose electrophoresis and purified using a gel purification kit (EZNA, VWR). The resulting amplicons, sequenced by Sanger method (Stabvida) were matched with the existing sequences using a PSI-Blast search.

Genetic organization of *ter* gene cluster

Organization of the *ter* operon was determined by PCR for the *Bacillus* strains 5W24, 3W19, ALJ98a and 10W7. Sets of primers for genes *terZ* and *terC* were designed based on the known sequences of *terZ*

and *terC* genes from *B. altitudinis* 3W19. Combinations of forward-reverse primers were designed to generate four sets of amplicons with primers from *terZ* and *terC*: terZ_F + terC_R, terZ_F + terC_F, terZ_R + terC_F and terZ_R + terC_R. The same combinations were performed with primers from *terC* and *telA*: telA_F + terC_R, telA_F + terC_F, telA_R + terC_F and telA_R + terC_R. Full list of PCR conditions can be seen in Supplementary Table S1.

Phylogenetic reconstruction and statistical analysis

Alignment of PCR amplified *ter* genes and closely related reference genes, obtained by PSI-Blast, was performed with ClustalW, and the phylogenetic reconstruction was performed using MegaX software package. All data presented in graphs is calculated with statistic based on three biological replicates, with standard deviations represented in error bars, and statistical significance is calculated, when applicable, using one-way ANOVA and Dunner's post-hoc test, using Prism, GraphPad10 software. Significant difference between experimental groups and control is represented as $*p \leq 0.05$, $**p \leq 0.01$ and $***p \leq 0.001$.